**The EMBO Journal** Vol.16 No.12 pp.3533–3543, 1997

# Minimal requirements for calcium oscillations driven by the $IP_3$ receptor

**György Hajnóczky and Andrew P.Thomas[1]**

Department of Pathology, Anatomy and Cell Biology,
Thomas Jefferson University, Philadelphia, PA 19107, USA

[1]Corresponding author
e-mail: thomasa@jeflin.tju.edu

**Hormones and neurotransmitters that act through inositol 1,4,5-trisphosphate ($IP_3$) can induce oscillations of cytosolic $Ca^{2+}$ ($[Ca^{2+}]_c$), which render dynamic regulation of intracellular targets. Imaging of fluorescent $Ca^{2+}$ indicators located within intracellular $Ca^{2+}$ stores was used to monitor $IP_3$ receptor channel ($IP_3R$) function and to demonstrate that $IP_3$-dependent oscillations of $Ca^{2+}$ release and re-uptake can be reproduced in single permeabilized hepatocytes. This system was used to define the minimum essential components of the oscillation mechanism. With $IP_3$ clamped at a submaximal concentration, coordinated cycles of $IP_3R$ activation and subsequent inactivation were observed in each cell. Cycling between these states was dependent on feedback effects of released $Ca^{2+}$ and the ensuing $[Ca^{2+}]_c$ increase, but did not require $Ca^{2+}$ re-accumulation. $[Ca^{2+}]_c$ can act at distinct stimulatory and inhibitory sites on the $IP_3R$, but whereas the $Ca^{2+}$ release phase was driven by a $Ca^{2+}$-induced increase in $IP_3$ sensitivity, $Ca^{2+}$ release could be terminated by intrinsic inactivation after $IP_3$ bound to the $Ca^{2+}$-sensitized $IP_3R$ without occupation of the inhibitory $Ca^{2+}$-binding site. These findings were confirmed using $Sr^{2+}$, which only interacts with the stimulatory site. Moreover, vasopressin induced $Sr^{2+}$ oscillations in intact cells in which intracellular $Ca^{2+}$ was completely replaced with $Sr^{2+}$. Thus, $[Ca^{2+}]_c$ oscillations can be driven by a coupled process of $Ca^{2+}$-induced activation and obligatory intrinsic inactivation of the $Ca^{2+}$-sensitized state of the $IP_3R$, without a requirement for occupation of the inhibitory $Ca^{2+}$-binding site.**

*Keywords*: $Ca^{2+}$ oscillations/endoplasmic reticulum/inositol 1,4,5-trisphosphate/$Sr^{2+}$ oscillations

## Introduction

One of the most common and fundamental mechanisms of cell signaling is through changes in the cytosolic free $Ca^{2+}$ concentration ($[Ca^{2+}]_c$) (Berridge, 1993; Clapham, 1995). The predominant pathway of $[Ca^{2+}]_c$ elevation in non-excitable cells is through the second messenger inositol 1,4,5-trisphosphate ($IP_3$), which mobilizes $Ca^{2+}$ from intracellular stores, most often associated with the endoplasmic or sarcoplasmic reticulum. The $[Ca^{2+}]_c$ signals generated in response to activation of receptors coupled to this signal transduction pathway are often complex at the single cell level, even when receptor activation occurs in a sustained and continuous manner. Thus, $IP_3$-linked agonists can give rise to large repetitive $[Ca^{2+}]_c$ transients, or oscillations, and each of these $[Ca^{2+}]_c$ transients may be organized at the subcellular level as a propagating $Ca^{2+}$ wave (Toescu, 1995; Thomas *et al.*, 1996). Studies using $Ca^{2+}$ indicator dyes within the intracellular stores of intact cells have shown that agonist-induced $[Ca^{2+}]_c$ oscillations are accompanied by inverse oscillations of stored $Ca^{2+}$ (Tse *et al.*, 1994; Chatton *et al.*, 1995). In many cases, the strength of the activating stimulus is conveyed to the cell by the frequency rather than the amplitude of the $[Ca^{2+}]_c$ oscillations, which has given rise to the concept of frequency-modulated $Ca^{2+}$ signaling (Berridge *et al.*, 1988; Goldbeter *et al.*, 1990). Although it is difficult to measure the output responses to these signals at the level of individual cells, it is clear that $[Ca^{2+}]_c$ oscillations represent an important mechanism in regulating cell function (Tse *et al.*, 1993; Hajnóczky *et al.*, 1995). The manifestation of $[Ca^{2+}]_c$ oscillations as $Ca^{2+}$ waves appears to reflect the subcellular organization of the $Ca^{2+}$ release system and the feedback interactions that give rise to the transient spikes of $[Ca^{2+}]_c$ increase (Toescu, 1995; Thomas *et al.*, 1996). Through these mechanisms, oscillatory $[Ca^{2+}]_c$ signals can be directed to discrete subcellular domains (Kasai *et al.*, 1993; Thorn *et al.*, 1993), propagate through entire cells (Rooney *et al.*, 1990; Lechleiter and Clapham, 1992) or even coordinate the activities of large numbers of coupled cells in intact tissues and organs (Stauffer *et al.*, 1993; Sanderson *et al.*, 1994; Robb-Gaspers and Thomas, 1995).

The mechanisms underlying $[Ca^{2+}]_c$ oscillations have been the subject of much study and of a number of reviews (Berridge, 1990, 1993; Petersen and Wakui, 1990; Meyer and Stryer, 1991; Thomas *et al.*, 1996). Most of the models describing $[Ca^{2+}]_c$ oscillations rely on positive and negative feedback effects on the $Ca^{2+}$ release system, resulting in either fluctuations in the level of $IP_3$ or changes in the activity of the $Ca^{2+}$ channels of the intracellular stores. It has been suggested that oscillations of $IP_3$ could arise from feedback activation of PLC by $[Ca^{2+}]_c$ (Harootunian *et al.*, 1991; Meyer and Stryer, 1991), and protein kinase C (PKC) has been proposed to function as a negative feedback regulator of $IP_3$ generation (Cobbold *et al.*, 1991). However, $[Ca^{2+}]_c$ oscillations can be induced by direct introduction of non-metabolizable $IP_3$ analogs in both mammalian cells (Wakui *et al.*, 1989) and in *Xenopus* oocytes (DeLisle and Welsh, 1992; Lechleiter and Clapham, 1992), suggesting that $[Ca^{2+}]_c$ oscillations are not secondary to oscillating levels of $IP_3$. An alternative mechanism of generating $IP_3$-dependent $[Ca^{2+}]_c$ oscillations has evolved from the observation that the $IP_3$ receptor $Ca^{2+}$ channel ($IP_3R$) is itself sensitive to both positive and negative feedback effects of $Ca^{2+}$ (Iino, 1990; Bezprozvanny *et al.*, 1991; Finch *et al.*, 1991).

© Oxford University Press

Thus, it has been proposed that each $[Ca^{2+}]_c$ transient is initiated by a local elevation of trigger $Ca^{2+}$ that activates $IP_3Rs$ in the immediate vicinity to yield the rapid rising phase of $Ca^{2+}$ release and propagation of $[Ca^{2+}]_c$ waves. This process is believed to be terminated by a negative feedback effect of the elevated $[Ca^{2+}]_c$ that inactivates the $IP_3R$ and allows the $Ca^{2+}$ pumps to re-sequester the released $Ca^{2+}$. Experiments in intact cells have provided evidence for both the positive and negative effects of $[Ca^{2+}]_c$ on the $IP_3R$ (Parker and Ivorra, 1990; DeLisle and Welsh, 1992; Lechleiter and Clapham, 1992; Oancea and Meyer, 1996), and regulation by luminal $Ca^{2+}$ has also been proposed (Missiaen *et al.*, 1991, 1992; Nunn and Taylor, 1992; Tanimura and Turner, 1996a). However, it is apparent that recovery from the inhibited state of the $IP_3R$ depends on factors other than the decline of $[Ca^{2+}]_c$ (Ilyin and Parker, 1994; Oancea and Meyer, 1996).

Previous studies of the mechanisms underlying $[Ca^{2+}]_c$ oscillations have relied on manipulations in intact cells, or have examined the individual components in isolation using subcellular systems. In the present study, we have established a permeabilized cell system in which $Ca^{2+}$ oscillations can be evoked by global application of $IP_3$. Repetitive cycles of $Ca^{2+}$ release and re-uptake were monitored using low affinity fluorescent $Ca^{2+}$ indicators localized within the intracellular $Ca^{2+}$ stores (Hofer and Machen, 1993, 1994), and changes in $IP_3R$ permeability were also monitored using the retrograde flux of $Mn^{2+}$ to quench luminal dye (Hajnóczky and Thomas, 1994; Hajnóczky *et al.*, 1994). This approach has allowed us to define the minimum requirements for intracellular $[Ca^{2+}]_c$ oscillations and dissect the mechanism in a single experimental system. $IP_3$-induced $Ca^{2+}$ oscillations were found to depend on fluctuations of $[Ca^{2+}]_c$, but $Ca^{2+}$ re-uptake and control by the luminal $Ca^{2+}$ content of the stores were not essential components of the mechanism. While this manuscript was in preparation, Tanimura and Turner (1996b) reported similar findings in salivary epithelial cells. In addition, we found that the $IP_3R$ undergoes an obligatory inactivation from the $Ca^{2+}$-sensitized state without the need for occupation of the inhibitory $Ca^{2+}$-binding site. Although this intrinsic inactivation is likely to occur together with $Ca^{2+}$-induced inhibition, experiments utilizing $Sr^{2+}$ in place of $Ca^{2+}$ suggest that the coupled processes of $Ca^{2+}$-dependent activation and subsequent obligatory inactivation of the $IP_3R$ is sufficient to generate $[Ca^{2+}]_c$ oscillations in intact cells without utilizing the inhibitory $Ca^{2+}$-binding site of the $IP_3R$.

## Results and discussion

### *$Ca^{2+}$ oscillations in intact and permeabilized hepatocytes*

Treatment of hepatocytes with vasopressin causes a dose-dependent generation of $IP_3$ (Thomas *et al.*, 1984), which is accompanied by $[Ca^{2+}]_c$ oscillations at submaximal agonist doses and sustained $[Ca^{2+}]_c$ increases with high levels of vasopressin (Figure 1A). The $[Ca^{2+}]_c$ oscillations in hepatocytes represent a very clear example of frequency modulation. The interspike period and initial latency decrease as the agonist dose is increased, but the amplitude and kinetics of the individual $[Ca^{2+}]_c$ spikes remain constant over a broad range of agonist doses (Woods *et al.*, 1986; Rooney *et al.*, 1989). The permeability of the intracellular $Ca^{2+}$ release channels during stimulation with vasopressin was monitored in intact hepatocytes by measuring the $Mn^{2+}$ quench of fura2 compartmentalized within the $Ca^{2+}$ stores (Glennon *et al.*, 1992; Hajnóczky *et al.*, 1993, 1994; Renard-Rooney *et al.*, 1993). Addition of submaximal vasopressin after pre-loading the cytosol with $Mn^{2+}$ resulted in a series of brief steps of rapid quench reflecting the opening of the intracellular channels, and these steps were separated by extended periods of slow quench where channel permeability was low (Figure 1B). The $Mn^{2+}$ quench steps and $[Ca^{2+}]_c$ oscillations showed similar sensitivities to vasopressin dose for latency and frequency, and high levels of vasopressin caused a sustained $Mn^{2+}$ quench that also paralleled the $[Ca^{2+}]_c$ response. Importantly, the rapid phase of $Mn^{2+}$ quench occurred with the same rate throughout the effective vasopressin dose range ($2.09 \pm 0.18$%/s and $2.11 \pm 0.09$%/s at 50 and 0.5 nM vasopressin, respectively). These data show that submaximal vasopressin doses cause synchronized periodic activation and subsequent deactivation of the entire population of intracellular $Ca^{2+}$ channels that can be activated by saturating levels of vasopressin. Thus, it appears that $[Ca^{2+}]_c$ oscillations in the intact cell are driven by cycling between a fully open and a largely closed state of the $IP_3R$ channels.

In order to dissect the mechanisms involved in this process, we established a permeabilized cell system that responds to a fixed level of exogenously added $IP_3$ with autonomous oscillations of $Ca^{2+}$ release and re-uptake at the single cell level. Hepatocytes were permeabilized with digitonin using a protocol that preserves the functional integrity of the endoplasmic reticulum (ER) $Ca^{2+}$ stores (Renard-Rooney *et al.*, 1993; Hajnóczky *et al.*, 1994). Luminal $[Ca^{2+}]$ ($[Ca^{2+}]_{ER}$) was measured with compartmentalized low affinity $Ca^{2+}$ indicators (fura2FF or furaptra) (Hofer and Machen, 1993, 1994). Submaximal doses of $IP_3$ evoked oscillations of $[Ca^{2+}]_{ER}$ that were inverted relative to vasopressin-induced $[Ca^{2+}]_c$ spikes in intact hepatocytes (Figure 1C). Thus, each $[Ca^{2+}]_{ER}$ spike consisted of a rapid $Ca^{2+}$ release phase followed by a slower re-accumulation of $Ca^{2+}$. The $[Ca^{2+}]_{ER}$ oscillations occurred in a coordinated manner throughout each cell, but adjacent cells in the imaging field responded asynchronously (Figure 2A). Stepped increases in $IP_3$ concentration increased the oscillation frequency, with little change in the kinetics or amplitude of the individual $[Ca^{2+}]_{ER}$ spikes (Figure 2B). The interspike period varied from 20 to 240 s, which is similar to the range observed for agonist-induced $[Ca^{2+}]_c$ oscillations in intact hepatocytes (Rooney *et al.*, 1989). Maximal doses of $IP_3$ caused a rapid and persistent loss of $[Ca^{2+}]_{ER}$ (Figures 1C and 2B). $Mn^{2+}$ quench of compartmentalized fura2 was also used to monitor changes in $IP_3R$ permeability during $IP_3$-induced $[Ca^{2+}]_{ER}$ oscillations in the permeabilized hepatocyte preparation. Consistent with the intact cell data (Figure 1B), submaximal doses of $IP_3$ evoked brief bursts of rapid $Mn^{2+}$ entry into the stores, separated by extended periods where $Mn^{2+}$ permeability returned close to the basal rate, whereas maximal $IP_3$ caused a sustained and complete quench of the luminal dye (Figure 1D). Taken together, these data demonstrate that the entire process responsible for $[Ca^{2+}]_c$ oscillations can be reproduced in

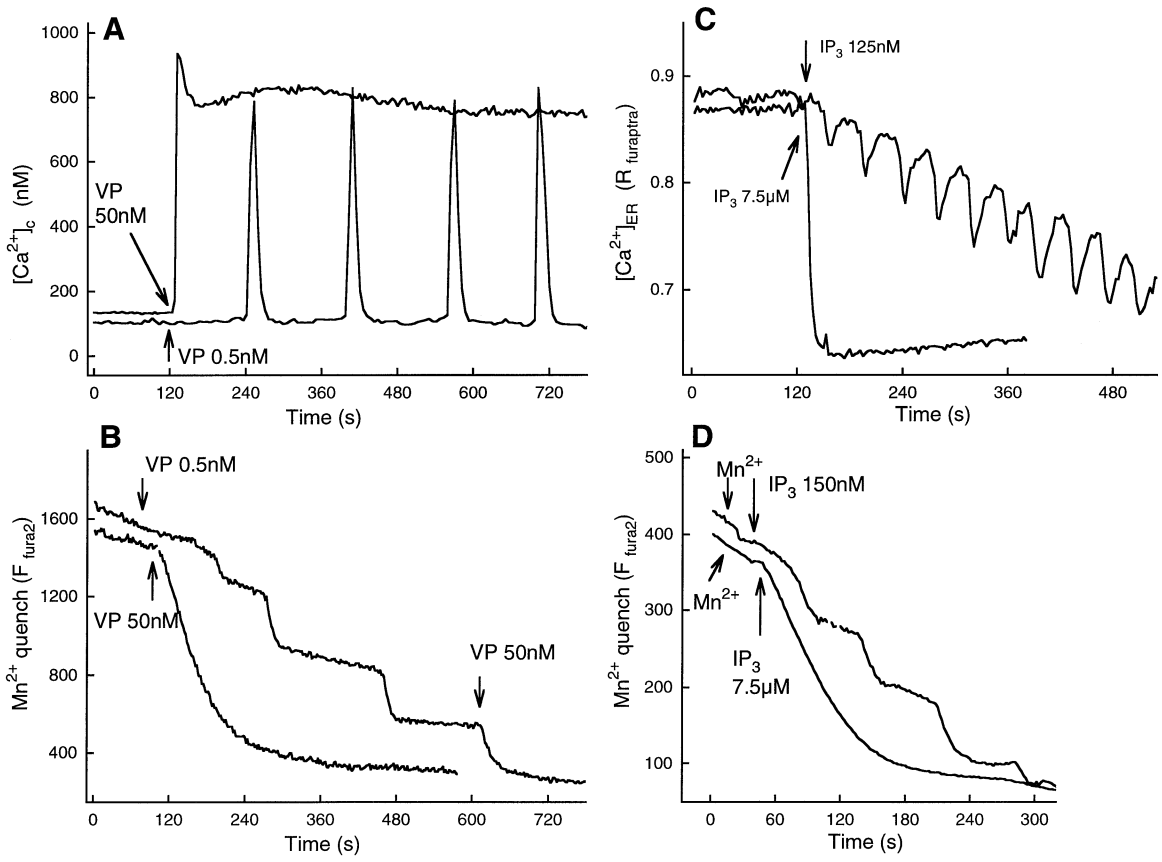


**Fig. 1.** Oscillations of $IP_3R$ permeability during $[Ca^{2+}]_c$ spikes in intact and permeabilized hepatocytes. (**A**) $[Ca^{2+}]_c$ responses to submaximal (0.5 nM) and maximal (50 nM) vasopressin (VP) monitored using cytosolic fura2 in single intact hepatocytes. Agonists were present continuously from the addition arrow. (**B**) Activation of intracellular $Ca^{2+}$ channels evoked by submaximal and maximal vasopressin monitored by $Mn^{2+}$ quench of compartmentalized fura2 in intact hepatocytes. Addition of 100 μM $MnCl_2$ to fura2-loaded hepatocytes resulted in rapid quench of the cytosolic dye (not shown), followed by slow quench of the compartmentalized dye. Extracellular $Mn^{2+}$ was washed out after complete quench of the cytosolic fura2 (prior to start of traces). The rate of quench reflects the penetration of $Mn^{2+}$ into the fura2-containing intracellular compartment. (**C**) Effects of submaximal (125 nM) and maximal (7.5 μM) $IP_3$ on $[Ca^{2+}]_{ER}$ were monitored using compartmentalized furaptra in single permeabilized hepatocytes. (**D**) $IP_3R$ activation by submaximal and maximal $IP_3$ was monitored as the $Mn^{2+}$ quench (50 μM $MnCl_2$) of compartmentalized fura2 in single permeabilized hepatocytes.

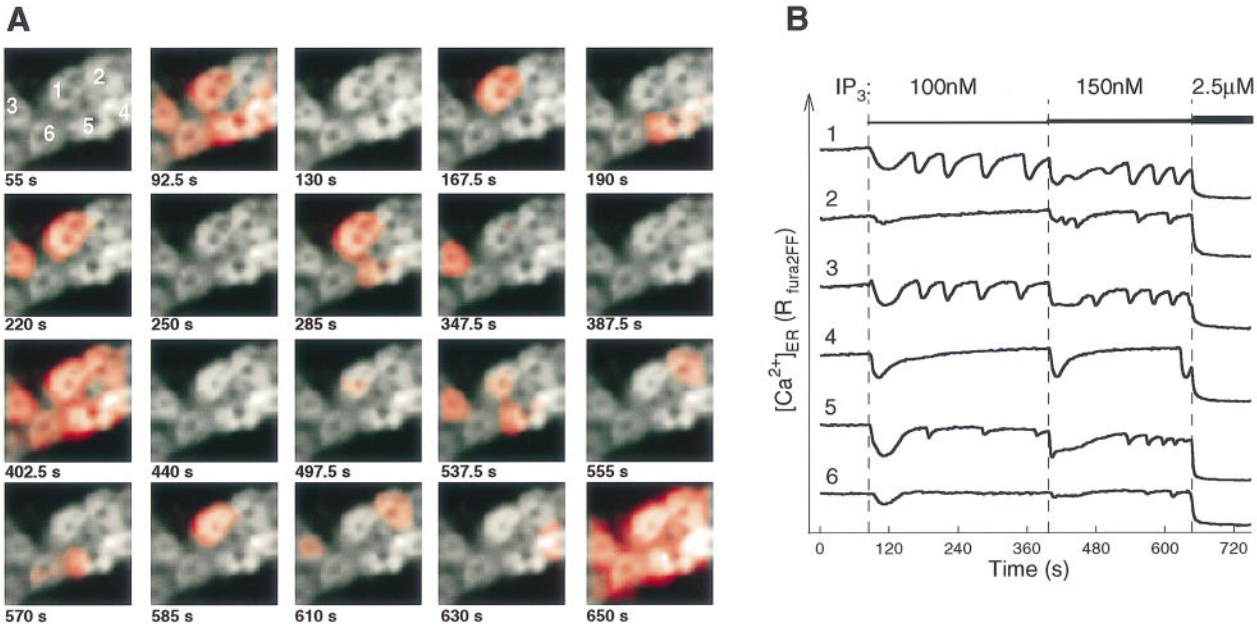


**Fig. 2.** Coordination and frequency modulation of $IP_3$-induced $[Ca^{2+}]_{ER}$ oscillations in single permeabilized hepatocytes. (**A**) Images of fura2FF-loaded permeabilized hepatocytes showing sites of $[Ca^{2+}]_{ER}$ decrease (red overlay) during $IP_3$-induced $[Ca^{2+}]_{ER}$ oscillations. The red overlay was calculated by differentiation of the images through time, using a step value of 6 s. (**B**) Time courses of $[Ca^{2+}]_{ER}$ change for numbered cells of (A) during incubation with 100 nM, 150 nM and 2.5 μM $IP_3$, as indicated.

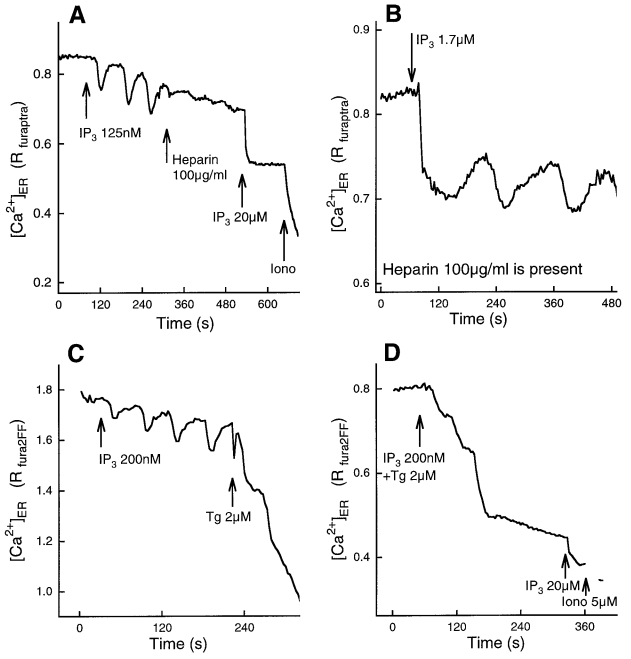


**Fig. 3.** Effects of heparin and thapsigargin on $IP_3$-induced oscillations of $[Ca^{2+}]_{ER}$. Fluorescence imaging was used to monitor $[Ca^{2+}]_{ER}$ in permeabilized hepatocytes loaded with furaptra (**A** and **B**) or fura2FF (**C** and **D**). Additions were made as indicated: Tg, thapsigargin; Iono, ionomycin. In (B), heparin (100 μg/ml) was added prior to the start.

a cell-free system in which the plasma membrane is disrupted and only the $Ca^{2+}$ fluxes mediated by intracellular organelles remain intact.

### *Mechanisms of permeabilized cell $Ca^{2+}$ oscillations*

Oscillations of $[Ca^{2+}]_{ER}$ occurred at a constant level of $IP_3$ applied in a bath volume >10 000-fold in excess of the original intracellular volume, suggesting that oscillatory changes of $[IP_3]$ were not required in this system. This is supported by experiments in which $[Ca^{2+}]_{ER}$ oscillations were induced by maximal $IP_3$ in the presence of the competitive $IP_3R$ blocker heparin (Ghosh *et al.*, 1988). In contrast to the stimulation of $IP_3$ binding by $[Ca^{2+}]_c$ (Pietri *et al.*, 1990), heparin affinity is not affected by $Ca^{2+}$ (Rouxel *et al.*, 1992), making it a good tool to shift the range of $IP_3$ sensitivity. Heparin addition terminated $[Ca^{2+}]_{ER}$ oscillations induced by submaximal $IP_3$ (Figure 3A). However, in the presence of heparin, $[Ca^{2+}]_{ER}$ oscillations could be observed with micromolar $IP_3$ concentrations that would otherwise cause sustained $[Ca^{2+}]_{ER}$ release (Figure 3B). Cellular formation or breakdown of $IP_3$ is unlikely to contribute significantly under these conditions, because $[IP_3]$ is effectively clamped at a high level. These findings are consistent with previous reports in which non-metabolizable $IP_3$ analogs induced $[Ca^{2+}]_c$ oscillations in intact cells (Wakui *et al.*, 1989; DeLisle and Welsh, 1992; Lechleiter and Clapham, 1992). A potential problem with the interpretation of the intact cell experiments is that there may be a contribution from oscillations of $IP_3$ formation secondary to the $Ca^{2+}$ release triggered by the non-metabolizable $IP_3$ analog. However, in our permeabilized cell studies, the presence of heparin would greatly reduce the efficacy of any endogenous $IP_3$ formation, which would also be diluted rapidly into the essentially infinite sink of extracellular medium containing high levels of exogenous $IP_3$.

One potential mechanism by which $[Ca^{2+}]_c$ oscillations could occur at a constant $IP_3$ level is through feedback regulation of the $IP_3R$ channel by $[Ca^{2+}]_{ER}$ (Missiaen *et al.*, 1991, 1992; Nunn and Taylor, 1992; Tanimura and Turner, 1996a). In this model, the cycling between open and closed states is dependent on both $Ca^{2+}$ release and re-uptake, such that inhibition of the ER $Ca^{2+}$ pump with thapsigargin would be expected to terminate the oscillations of $[Ca^{2+}]_{ER}$. When thapsigargin was added either during $IP_3$-induced $[Ca^{2+}]_{ER}$ oscillations (Figure 3C) or together with $IP_3$ (Figure 3D), the re-uptake phase of the $[Ca^{2+}]_{ER}$ spikes was completely prevented. However, $Ca^{2+}$ release still occurred in a periodic manner and, as a result, $[Ca^{2+}]_{ER}$ declined in a series of discrete steps. The $Mn^{2+}$ quench approach (see Figure 1D) also showed the same cycling between the high and low permeability states of the $IP_3R$ when thapsigargin was added shortly before $IP_3$ under these conditions (data not shown). Thus, feedback regulation by $[Ca^{2+}]_{ER}$ is not an essential component of the $Ca^{2+}$ oscillation mechanism.

The role of $[Ca^{2+}]_c$ in the permeabilized hepatocyte system was investigated using 10 mM BAPTA to buffer the medium $Ca^{2+}$ ($[Ca^{2+}]_o$). Under these conditions, the bell-shaped dependence on $[Ca^{2+}]_c$ (Iino, 1990; Bezprozvanny *et al.*, 1991; Finch *et al.*, 1991) was clearly apparent at submaximal $IP_3$, with properties similar to those described previously for hepatocytes permeabilized in suspension (Marshall and Taylor, 1993). For example, at 250 nM $IP_3$, the rate of $[Ca^{2+}]_{ER}$ release was stimulated 15 ± 6-fold when $[Ca^{2+}]_o$ was increased from <5 to 500 nM, whereas $Ca^{2+}$ release rates decreased with higher $[Ca^{2+}]_o$ and were barely detectable at >5 μM $[Ca^{2+}]_o$ (not shown). $IP_3$ released $Ca^{2+}$ throughout the range of 1–2000 nM $[Ca^{2+}]_o$, but $[Ca^{2+}]_{ER}$ oscillations were never observed in the presence of the $Ca^{2+}$ buffer (e.g. Figure 4A), indicating that fluctuations in $[Ca^{2+}]_o$ are necessary for $[Ca^{2+}]_{ER}$ oscillations. Although the $Ca^{2+}$ buffer prevented oscillations, $Ca^{2+}$ release induced by submaximal $IP_3$ was still transient at $[Ca^{2+}]_o$ levels >200 nM (Figure 4A). Since $[Ca^{2+}]_o$ was highly buffered, $Ca^{2+}$ re-uptake reflects refilling of the same $Ca^{2+}$ store at steady-state, which implies an inactivation of the $IP_3R$ channel sufficient to allow the ER $Ca^{2+}$ pump to overcome the $IP_3$-activated release pathway. This was demonstrated directly by addition of thapsigargin at steady-state, which revealed a $Ca^{2+}$ release rate >10-fold slower than the rate when $IP_3$ was added initially or when $IP_3$ and thapsigargin were added simultaneously to naive cells (Figure 4A). By contrast, $Ca^{2+}$ release rates recovered when $IP_3$ was washed out and then added again (Figure 4B). The high level of BAPTA makes it unlikely that steady-state inactivation of the $IP_3R$ was mediated by released $Ca^{2+}$ during sustained incubation with $IP_3$. An alternative to $Ca^{2+}$ feedback inhibition that might contribute to the decline in $Ca^{2+}$ release under these conditions is the ligand-induced inactivation of the $IP_3R$ by $IP_3$, which occurs in a time-dependent manner at fixed $[Ca^{2+}]_o$ (Hajnóczky and Thomas, 1994).

### *Role of $IP_3$-induced inactivation of the $IP_3R$*

The time-dependent inactivation of the $IP_3R$ by $IP_3$ was demonstrated originally by measuring $IP_3R$ permeability

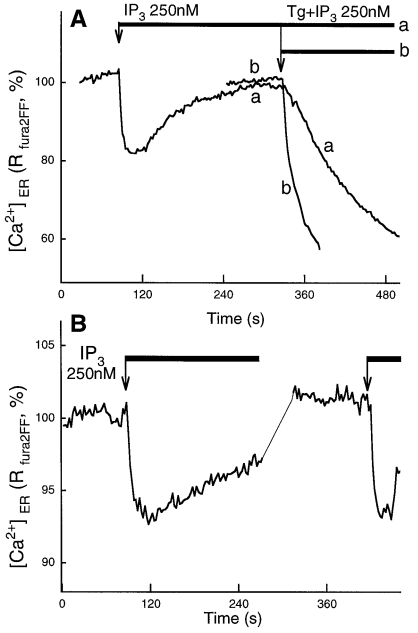


**Fig. 4.** Transient $[Ca^{2+}]_{ER}$ release by $IP_3$ in the presence of $Ca^{2+}$-BAPTA buffer. Permeabilized fura2FF-loaded hepatocytes were incubated in intracellular medium supplemented with 10 mM Na-BAPTA (Calbiochem) and 7.5 mM $CaCl_2$, giving a measured $[Ca^{2+}]_o$ of ~800 nM calibrated with fura2 (using $K_d$ = 220 nM). Ruthenium red was also included to block mitochondrial $Ca^{2+}$ uptake. (**A**) Cells were first incubated with 250 nM $IP_3$ and then 4 μM thapsigargin (Tg) was added once $[Ca^{2+}]_{ER}$ had returned to a steady-state in the continuous presence of $IP_3$ (trace a), or $IP_3$ and thapsigargin were added simultaneously (trace b). Traces are averaged from the entire cell population in the imaging field (30–50 cells). (**B**) Cells were incubated with 250 nM $IP_3$, followed by washout (three changes of medium) and then readdition of the same level of $IP_3$ where indicated.

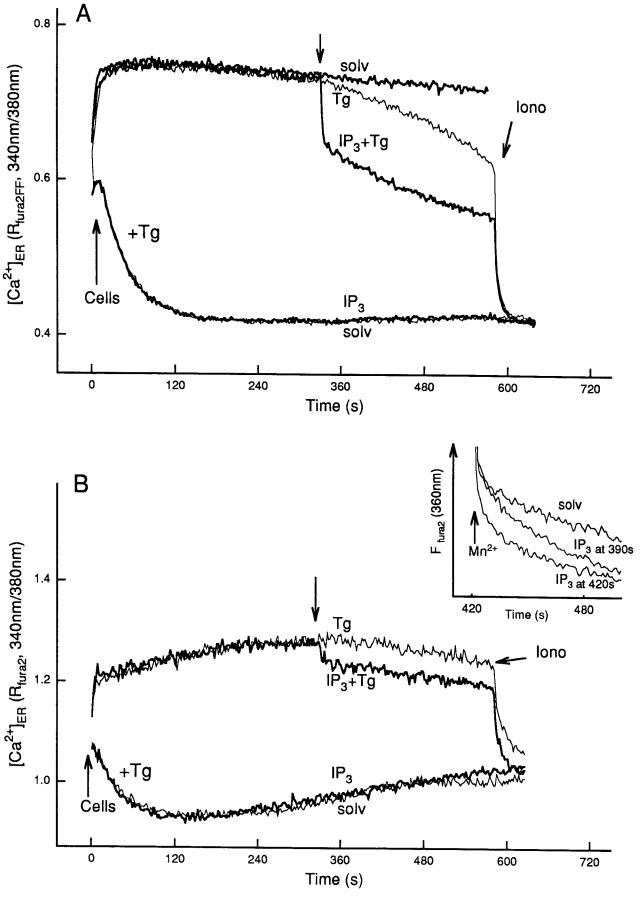


**Fig. 5.** Effect of thapsigargin pre-treatment on $IP_3$-induced changes in $[Ca^{2+}]_{ER}$. Suspensions of hepatocytes loaded with fura2FF (**A**) or fura2 (**B**) were permeabilized in ICM supplemented with 15 mM Na-BAPTA and 9 mM $CaCl_2$, giving a measured $[Ca^{2+}]_o$ of ~400 nM calibrated with fura2. Ruthenium red was also included to block mitochondrial $Ca^{2+}$ uptake. Other additions were 2 μM thapsigargin (Tg), 12.5 μM $IP_3$, 10 μM ionomycin (Iono) or solvent (solv), as indicated. The inset to (B) shows $Mn^{2+}$ quench measurements for fura2-loaded hepatocytes permeabilized in ICM (~400 nM $[Ca^{2+}]_o$) supplemented with 2 μM thapsigargin. Fluorescence quenching was initiated 420 s after permeabilization by addition of 40 μM $MnCl_2$ in the absence of $IP_3$ (solv), after 30 s pre-incubation with 12.5 μM $IP_3$ ($IP_3$ at 390 s) or with $IP_3$ added together with the $MnCl_2$ ($IP_3$ at 420 s).

using retrograde $Mn^{2+}$ flux through the channel to quench luminal fura2 at various times after addition of $IP_3$ (Hajnóczky and Thomas, 1994). In those experiments, suspensions of permeabilized hepatocytes were pre-incubated with thapsigargin to deplete the $Ca^{2+}$ stores. However, Combettes *et al.* (1996) suggested recently that there may have been sufficient residual $Ca^{2+}$ within the stores under these conditions to sensitize the $IP_3R$ to $IP_3$, and that loss of this $[Ca^{2+}]_{ER}$ during the incubation with $IP_3$ could account for the inactivation of the $IP_3R$. Although we observed no $Ca^{2+}$ release and no change in $[Ca^{2+}]_{ER}$ measured with luminal fura2 in response to $IP_3$ in thapsigargin-treated cells in our previous studies (Hajnóczky and Thomas, 1994), we have re-examined this question using both low and high affinity $Ca^{2+}$ indicator dyes. In the present experiments, suspensions of hepatocytes were permeabilized in the presence or absence of 2 μM thapsigargin with $[Ca^{2+}]_o$ buffered to 400 nM with 15 mM BAPTA. When $[Ca^{2+}]_{ER}$ was monitored with luminal fura2FF (Figure 5A), inclusion of thapsigargin from the start of the experiment (lower two traces of Figure 5A) completely blocked $Ca^{2+}$ uptake and depleted the $Ca^{2+}$ stores to the point where $IP_3$ was unable to cause any further loss of $[Ca^{2+}]_{ER}$. Thapsigargin was less effective in depleting the $Ca^{2+}$ stores when added after completion of ATP-dependent $Ca^{2+}$ uptake (upper traces of Figure 5A), but treatment with ionomycin caused a rapid decrease of $[Ca^{2+}]_{ER}$ to the level measured in cells pre-treated with thapsigargin. Pre-incubation with thapsigargin was also found to eliminate the $Ca^{2+}$ release response to $IP_3$ in experiments using luminal fura2, which has the advantage of being sensitive to $[Ca^{2+}]_{ER}$ in the submicromolar range (Figure 5B).

The same fura2-loaded cell preparation examined in Figure 5B was also used for $Mn^{2+}$ quench measurements of $IP_3R$ permeability (Figure 5B inset). These experiments demonstrate that the initial fast phase of $Mn^{2+}$ quenching observed when $IP_3$ was added together with the $Mn^{2+}$ was greatly reduced when the cells were pre-incubated with $IP_3$ for 30 s. This reflects the time-dependent inactivation induced by $IP_3$, as reported previously (Hajnóczky and Thomas, 1994). These findings also provide direct evidence that the $IP_3R$ remains permeable to $Mn^{2+}$ even when the stores are completely depleted of $Ca^{2+}$, in contrast to the findings of Tanimura and Turner (1996a). Another potential problem with the use of $Mn^{2+}$ to study $IP_3R$ permeability is that $Mn^{2+}$ may displace $Ca^{2+}$ from other binding sites, which could then contribute to the inhibition

of the $IP_3R$ (Combettes *et al.*, 1996). However, the presence of 2 mM Mg-ATP in our experiments provides additional $Ca^{2+}$ and $Mn^{2+}$ buffering capacity, which prevents the substantial $Ca^{2+}$ changes that might otherwise occur on $Mn^{2+}$ addition (calculated $[Ca^{2+}]_o$ increased from 435 to 515 nM after $MnCl_2$ addition in Figure 5B). Moreover, this $[Ca^{2+}]_o$ change occurs only at the time of $Mn^{2+}$ addition, and so cannot explain the time-dependent decrease in $Mn^{2+}$ uptake rate during pre-incubation of the cells with $IP_3$. It should also be noted that Striggow and Ehrlich (1996) have concluded that the free $[Mn^{2+}]$ used in these experiments (2 μM) is close to the optimum for measuring $IP_3R$ permeability.

Since the $Ca^{2+}$ dependence for sensitization of the $IP_3R$ to $IP_3$ and for $IP_3$-dependent inactivation appeared to be similar in hepatocytes (Marshall and Taylor, 1993; Hajnóczky and Thomas, 1994), we hypothesized that these may be coupled events. Therefore, the $Mn^{2+}$ quench approach was used to compare the effects of $[Ca^{2+}]_o$ on $IP_3R$ sensitization and $IP_3$-induced inactivation in suspensions of fura2-loaded hepatocytes permeabilized in the presence of thapsigargin. The $Mn^{2+}$ quench evoked by 125 nM $IP_3$ was taken as a measure of $IP_3R$ sensitization, and the inhibition of $Mn^{2+}$ quench evoked by maximal $IP_3$ after a 20 s pre-pulse with either 125 nM or 7.5 μM $IP_3$ was used to measure $IP_3$-dependent inactivation (Hajnóczky and Thomas, 1994). In addition, the $[Ca^{2+}]_o$-induced increase in the proportion of high affinity $IP_3Rs$ was measured using a low level of $[^3H]IP_3$ (Pietri *et al.*, 1990; Marshall and Taylor, 1994). There was a very marked increase in $IP_3R$ channel activation by 125 nM $IP_3$ as $[Ca^{2+}]_o$ was increased in the range 300 nM to 1 μM (Figure 6A), and this was paralleled by a dramatic increase in $IP_3$-induced inactivation (Figure 6B). The $[Ca^{2+}]_o$ dependence of activation and inactivation at submaximal $IP_3$ was shifted to higher $[Ca^{2+}]_o$ than the sensitization for $IP_3$ binding (Figure 6C), which may result from the cooperative nature of channel activation at submaximal $IP_3$ (Meyer *et al.*, 1990). Although maximal $IP_3$ caused $IP_3R$ activation at all levels of $[Ca^{2+}]_o$, the extent of inactivation was entirely dependent on $[Ca^{2+}]_o$ and was closely correlated with the $[Ca^{2+}]_o$-induced increase in high affinity $IP_3$ binding (Figure 6A–C).

The correlation between $IP_3R$ sensitization and inactivation was investigated further by substituting $Sr^{2+}$ and $Ba^{2+}$ for $Ca^{2+}$. Marshall and Taylor (1994) have shown that the sensitizing effects of $Ca^{2+}$ on $IP_3$ binding and $Ca^{2+}$ release are mimicked by $Sr^{2+}$ but not by $Ba^{2+}$, and that neither $Sr^{2+}$ nor $Ba^{2+}$ is effective in mimicking the direct inhibitory effect of $Ca^{2+}$. To eliminate the potential for feedback by released $Ca^{2+}$, the effects of $Sr^{2+}$ and $Ba^{2+}$ on $IP_3R$ channel activation were monitored by the $IP_3$-induced retrograde flux of these ions into fura2-loaded stores in the presence of thapsigargin and EGTA. $Sr^{2+}$ caused a marked sensitization to $IP_3$ (50 nM) compared with $Ba^{2+}$ (Figure 7A), and this can be explained by the differential effects of these ions on $IP_3$ binding under these conditions (Figure 7C, and see Marshall and Taylor, 1994). These effects on $IP_3$ sensitivity were paralleled by $IP_3$-induced inactivation, such that $Sr^{2+}$ but not $Ba^{2+}$ supported the time-dependent inactivation during $IP_3$ pre-incubation (Figure 7B). The fact that $Ba^{2+}$ was without effect shows that $Sr^{2+}$ was not acting simply by displacing

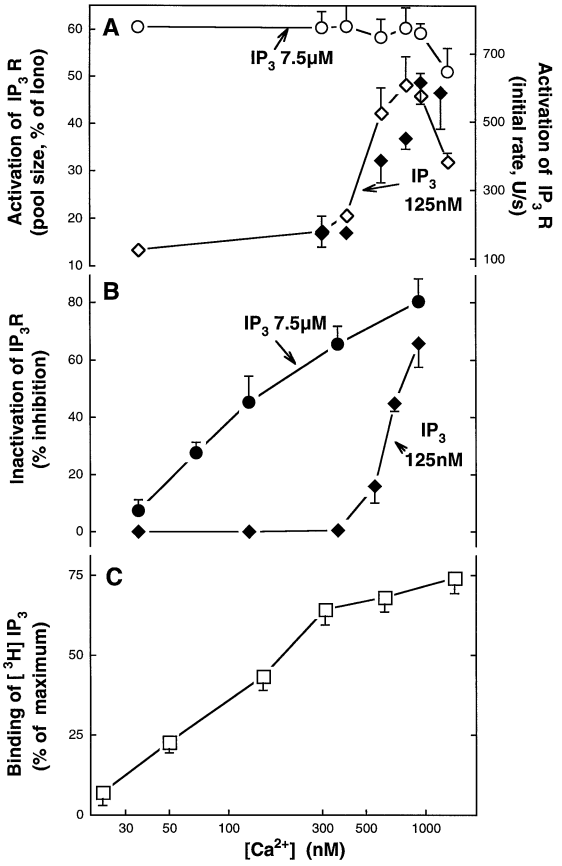


**Fig. 6.** Effects of $[Ca^{2+}]_o$ on $IP_3R$ activation, inactivation and $IP_3$ binding. (**A**) The effect of $[Ca^{2+}]_o$ on $IP_3R$ activation by submaximal (125 nM) and maximal (7.5 μM) $IP_3$ was measured as the $Mn^{2+}$ quench of compartmentalized fura2 in suspensions of permeabilized hepatocytes. Initial rates of $Mn^{2+}$ quench (arbitrary units) were measured over the first 3 s after $IP_3$ addition (closed symbols). The $IP_3$-sensitive pool size (open symbols) was normalized to the total ionomycin-sensitive compartment. (**B**) $IP_3$-induced inactivation was measured by pre-incubation with 125 nM or 7.5 μM $IP_3$ for 20 s prior to addition of $Mn^{2+}$ and maximal $IP_3$, essentially as shown in the inset to Figure 5B. The component of inactivation due to pre-incubation with $IP_3$ was calculated as the decrease in $Mn^{2+}$ quench rate compared with the rate of quench when $IP_3$ and $Mn^{2+}$ were added to cells pre-incubated in the absence of $IP_3$ at the same level of $[Ca^{2+}]_o$. (**C**) Effect of $[Ca^{2+}]_o$ on $[^3H]IP_3$ binding.

$Ca^{2+}$ from other binding sites. Thus, the differential effects of $Sr^{2+}$ and $Ba^{2+}$ on $IP_3$-induced inactivation indicate that the $Ca^{2+}$ dependence of this process reflects binding to the stimulatory $Ca^{2+}$ site of the $IP_3R$.

Taken together, the data of Figures 6 and 7 provide evidence that only the $Ca^{2+}$- (or $Sr^{2+}$-) sensitized form of the $IP_3R$ undergoes ligand-induced inactivation. Moreover, the fact that $Sr^{2+}$ is effective in supporting $IP_3$-induced inactivation indicates that this process does not depend on divalent metal ion binding at the inhibitory site of the $IP_3R$. Finally, the observation that inactivation at submaximal $[IP_3]$ follows a similar cooperative $Ca^{2+}$ dependence to activation (Figure 6A and B) but does not parallel the non-cooperative $Ca^{2+}$ dependence of $IP_3$ binding suggests that channel opening is a prerequisite for the inactivation process and hence inactivation may be an obligatory consequence of channel activation in the $Ca^{2+}$-sensitized state.

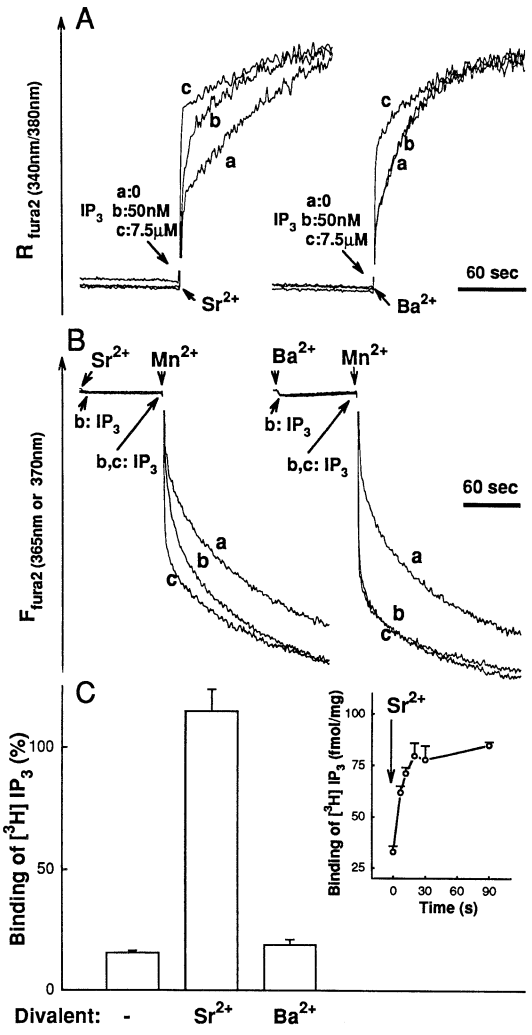


**Fig. 7.** Effects of $Sr^{2+}$ and $Ba^{2+}$ on $IP_3R$ activation and inactivation. (**A**) Effect of $Sr^{2+}$ and $Ba^{2+}$ on $IP_3R$ activation by submaximal and maximal $IP_3$ measured as the retrograde flux of each divalent cation from the medium and detected with compartmentalized fura2. Traces show (a) no $IP_3$, (b) 50 nM $IP_3$ and (c) 7.5 μM $IP_3$. (**B**) Effect of $Sr^{2+}$ and $Ba^{2+}$ on $IP_3R$ inactivation induced by pre-treatment with $IP_3$, measured as the $Mn^{2+}$ quench of compartmentalized fura2. Traces show (a) no $IP_3$, (b) 7.5 μM $IP_3$ added 90s before $Mn^{2+}$ and (c) 7.5 μM $IP_3$ added simultaneously with $Mn^{2+}$. (**C**) Effects of $Sr^{2+}$ and $Ba^{2+}$ on steady-state $IP_3$ binding; the inset shows the time course of the $Sr^{2+}$ effect (50 nM [$^3$H]$IP_3$). For these experiments, hepatocytes were permeabilized in ICM without MgATP and supplemented with 40 μM EGTA and 2 μM thapsigargin to prevent $Ca^{2+}$ uptake. In (A) and (C), 200 μM $SrCl_2$ and 140 μM $BaCl_2$ were added, giving ~160 μM free $Sr^{2+}$ and ~100 μM free $Ba^{2+}$. For (B), $SrCl_2$ and $BaCl_2$ were both added at 100 μM and quenching was initiated with 100 μM $MnCl_2$. The initial rapid phase in the control traces (a) of (A) and (B) reflects fluorescence responses of cytosolic dye that was released to the medium during permeabilization.

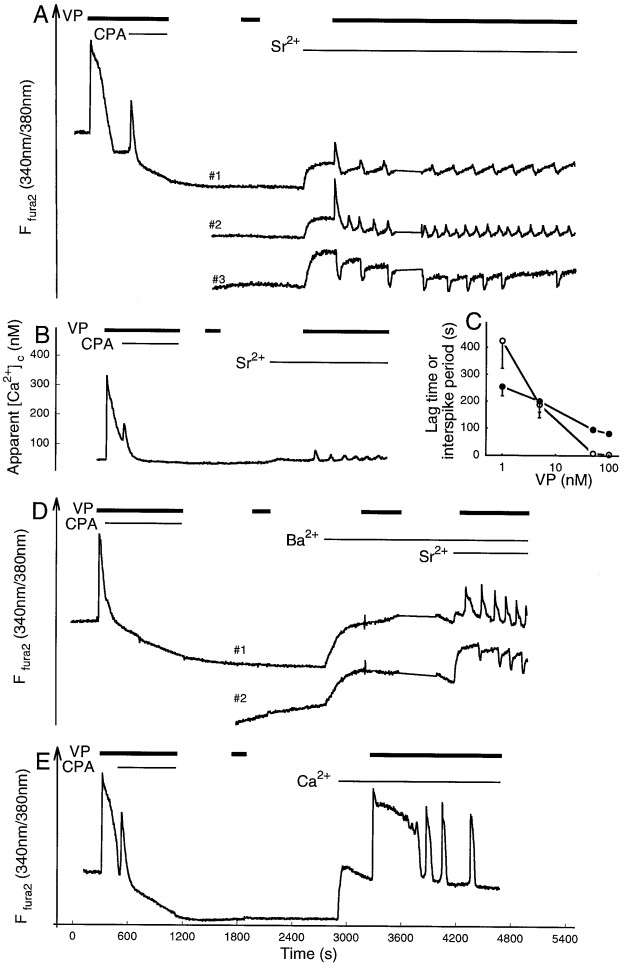


**Fig. 8.** $Sr^{2+}$ oscillations in single hepatocytes. Fura2-loaded hepatocytes were incubated in $Ca^{2+}$-free ECM supplemented with 0.5 mM Na-EGTA. The cells were first treated with maximal vasopressin (100 nM, VP) and cyclopiazonic acid (200 μM) to deplete intracellular $Ca^{2+}$ stores. These agents were then washed out (4–5 changes of medium) and the cells stimulated a second time with 100 nM vasopressin. After a second washout period, the medium was supplemented with 3 mM $SrCl_2$, 3 mM $BaCl_2$ or 2 mM $CaCl_2$, as indicated, and the cells subsequently challenged again with vasopressin. Fura2 was loaded as fura2/AM for (**A**), (**D**) and (**E**) and was microinjected as the free acid form for (**B**). The downward spikes in the presence of $Sr^{2+}$ in (A) and (D) represent the decrease of $[Sr^{2+}]_{ER}$ in cells in which compartmentalized dye predominated. (**C**) Vasopressin dose–response data for the initial lag time (○) and interspike period (●) for $Sr^{2+}$ oscillations in fura2/AM-loaded hepatocytes. Cells giving sustained $Sr^{2+}$ increases in response to vasopressin were omitted from the frequency analysis, but the proportion of these increased with vasopressin dose: specifically 0, 30, 44 and 57% of cells gave sustained $Sr^{2+}$ responses at 1, 5, 50 and 100 nM vasopressin, respectively.

### *Agonist-induced oscillations of $[Sr^{2+}]_c$ in intact hepatocytes*

The data presented above and previous studies comparing the effects of divalent metal ions on $IP_3R$ function suggested that $Sr^{2+}$ could be used to distinguish the roles of $IP_3$-dependent inactivation of the $IP_3R$ and direct feedback inhibition by $Ca^{2+}$ in the generation of $[Ca^{2+}]_c$ oscillations in intact cells. It has been shown that $Sr^{2+}$ can be accumulated by ATP-dependent intracellular $Ca^{2+}$ stores and subsequently released in response to agonist (Montero *et al.*, 1995). In order to eliminate possible contributions to $IP_3R$ regulation from residual $Ca^{2+}$ in the stores (Morgan and Jacob, 1996), hepatocytes were incubated in the presence of EGTA and treated with high vasopressin and the reversible SERCA $Ca^{2+}$ pump inhibitor cyclopiazonic acid (Figure 8). After washout of these agents, there was no further $[Ca^{2+}]_c$ response to vasopressin. Following a further washout period, the cells were exposed to $SrCl_2$, $BaCl_2$ or $CaCl_2$, each of which rapidly appeared in the cytosol, presumably as a result of the activated capacitative $Ca^{2+}$ entry pathway. The cells were allowed to re-load with the added divalent cation and, after a steady-state was

achieved, they were challenged again with vasopressin. Vasopressin-induced oscillations of fura2 fluorescence were observed in the cells re-loaded with $Sr^{2+}$ and $Ca^{2+}$, but not in those loaded with $Ba^{2+}$. Although $Ba^{2+}$ did not support oscillations, it did not prevent the induction of oscillations by vasopressin when the medium was supplemented with $SrCl_2$ in the continuing presence of $BaCl_2$.

Loading of hepatocytes with fura2 acetoxymethyl ester (fura2/AM) results in partial compartmentalization of the dye in the ER. This luminal fura2 does not usually contribute to the measured $[Ca^{2+}]_c$ changes in intact cells, because $[Ca^{2+}]_{ER}$ remains sufficiently high to saturate the dye unless the cells are treated with agonist in the presence of SERCA pump inhibitors (Glennon *et al*., 1992). However, the affinity of fura2 for $Sr^{2+}$ is 30-fold lower than for $Ca^{2+}$ and, as a result, the oscillations of fura2 fluorescence recorded in the presence of $Sr^{2+}$ reflect a mixed signal for the cytosolic and ER compartments. This gave rise to a variety of oscillation patterns, ranging from largely cytosolic signals (Figure 8A, cell #2, and D, cell #1) to those cells in which the luminal changes predominate (Figure 8A, cell #3, and D, cell #2). Microinjected fura2 was used to obtain a pure cytosolic signal (Figure 8B). In these experiments, vasopressin gave rise to baseline spikes in the $Sr^{2+}$-loaded cells that propagated throughout the cell and were similar to those observed with $Ca^{2+}$, except the $[Sr^{2+}]_c$ oscillations were 10- to 20-fold smaller in amplitude than the $[Ca^{2+}]_c$ oscillations in the same cells. This can be explained by the lower affinity of fura2 for $Sr^{2+}$, and suggests that the absolute magnitude of $[Ca^{2+}]_c$ and $[Sr^{2+}]_c$ oscillations are similar in hepatocytes. The $Sr^{2+}$ oscillations also demonstrated frequency modulation, such that the initial lag time and the interspike period decreased with increasing vasopressin dose (Figure 8C).

The fact that the cells were incubated in the presence of EGTA and depleted of $Ca^{2+}$ to the point where there was no detectable $Ca^{2+}$ release to vasopressin should ensure that the oscillations in $Sr^{2+}$-loaded cells are due predominantly to $Sr^{2+}$ fluxes. A number of other lines of evidence support the conclusion that these are $Sr^{2+}$ oscillations and that they are driven directly by $Sr^{2+}$ feedback effects rather than as a secondary consequence of residual $Ca^{2+}$ fluxes. The observation of oscillatory decreases in $[Sr^{2+}]_{ER}$ in fura2/AM-loaded cells indicates that $[Ca^{2+}]_{ER}$ must have been reduced to the submicromolar range where it was no longer able to saturate the luminal fura2. Furthermore, $Sr^{2+}$-dependent oscillations continued for >30 min, often with little change in amplitude through many cycles. This repetitive cycling would be expected to chase out any residual $Ca^{2+}$ that could play a role in feedback regulation at the $IP_3R$. Finally, the small amplitudes of the oscillations measured with microinjected cytosolic fura2 are consistent with $[Sr^{2+}]_c$ spikes, whereas if these reflected $[Ca^{2+}]_c$ spikes they would be inadequate to elicit the feedback activation of the $IP_3R$ necessary to propagate the release throughout the cell. The small amplitude of these spikes also shows that $[Sr^{2+}]_c$ does not achieve the near millimolar concentrations where it might act at the inhibitory $Ca^{2+}$ site of the $IP_3R$ (Marshall and Taylor, 1994). We were unable to determine whether $Sr^{2+}$ alone could support $IP_3$-induced oscillations in our permeabilized cell system, because we cannot use chelators in this preparation, and the contaminating $Ca^{2+}$ and effectively infinite volume of the incubation medium are sufficient to allow substantial $Ca^{2+}$ loading of the intracellular stores. Nevertheless, the observation of $[Sr^{2+}]_c$ oscillations in intact cell experiments and the demonstration that $Sr^{2+}$ mimics the effects of $Ca^{2+}$ in sensitizing the $IP_3R$ and supporting $IP_3$-dependent inactivation in permeabilized cells provides strong evidence that $Sr^{2+}$ is able to substitute effectively for $Ca^{2+}$ in driving the basic oscillation mechanism. Moreover, the inability of $Sr^{2+}$ to substitute for $Ca^{2+}$ at the inhibitory binding site of the $IP_3R$ suggests that this form of negative feedback control by $Ca^{2+}$ is not essential to obtain $[Ca^{2+}]_c$ oscillations.

### Conclusions

Our findings with permeabilized hepatocytes demonstrate that feedback regulation of the $IP_3R$ by $[Ca^{2+}]_c$ at a constant level of $IP_3$ represents the minimum requirement for oscillatory $Ca^{2+}$ release. In addition, it appears that the stimulatory $Ca^{2+}$-binding site of the $IP_3R$ can effect both activation and termination of $Ca^{2+}$ release, with the latter process occurring through the intrinsic slow inactivation that follows $IP_3$-induced activation of the $Ca^{2+}$-sensitized state of the $IP_3R$. This does not exclude an additional contribution from direct negative feedback by released $Ca^{2+}$ at the inhibitory $Ca^{2+}$-binding site. It is also difficult to formally exclude the possibility that $IP_3$ binding to the $Ca^{2+}$-sensitized $IP_3R$ leads to a change in the properties of the inhibitory $Ca^{2+}$-binding site that increases its affinity for $Ca^{2+}$, and perhaps $Sr^{2+}$. It is possible that other regulatory mechanisms may also contribute to $[Ca^{2+}]_c$ oscillations in intact cells, including regulation of the $IP_3R$ by $[Ca^{2+}]_{ER}$, $[Ca^{2+}]_c$ stimulation of $IP_3$ formation and enhanced plasma membrane $Ca^{2+}$ entry. However, our findings in the permeabilized cell preparation demonstrate that these are not essential components of the $[Ca^{2+}]_c$ oscillator.

Our studies suggest a basic mechanism of $[Ca^{2+}]_c$ oscillations that depends on $[Ca^{2+}]_c$-dependent interconversion between two modes of $IP_3R$ channel activation, a $Ca^{2+}$-free basal state that requires high levels of $IP_3$ for activation and a $Ca^{2+}$-sensitized state that can be activated at much lower levels of $IP_3$ but undergoes an intrinsic inactivation when $IP_3$ is bound. The $Ca^{2+}$- (and $Sr^{2+}$-) dependent interconversions of the $IP_3R$ are shown in Figure 9, with the postulated predominant pathway underlying a $[Ca^{2+}]_c$ spike shown by the thick blue arrows. At the resting $[Ca^{2+}]_c$ between $[Ca^{2+}]_c$ spikes, $IP_3$ affinity is low and the $IP_3R$ channel does not inactivate, so that submaximal levels of $IP_3$ cause continuous low level $Ca^{2+}$ release. As $[Ca^{2+}]_c$ rises, $IP_3Rs$ convert to a conformation with high affinity for $IP_3$, which accelerates $Ca^{2+}$ release by these channels resulting in positive feedback by $[Ca^{2+}]_c$ that effectively recruits all available $IP_3Rs$ to the high affinity activated conformation. A key observation of the present study is that there is an obligatory coupling between channel opening and inactivation in the $Ca^{2+}$-sensitized state of the $IP_3R$. Thus, in the high affinity conformation, $IP_3R$ activation occurs in a phasic manner, whereby channel opening is followed by a time-dependent inactivation that does not require further $Ca^{2+}$ binding. An obligatory linkage between the activation and inactiv-

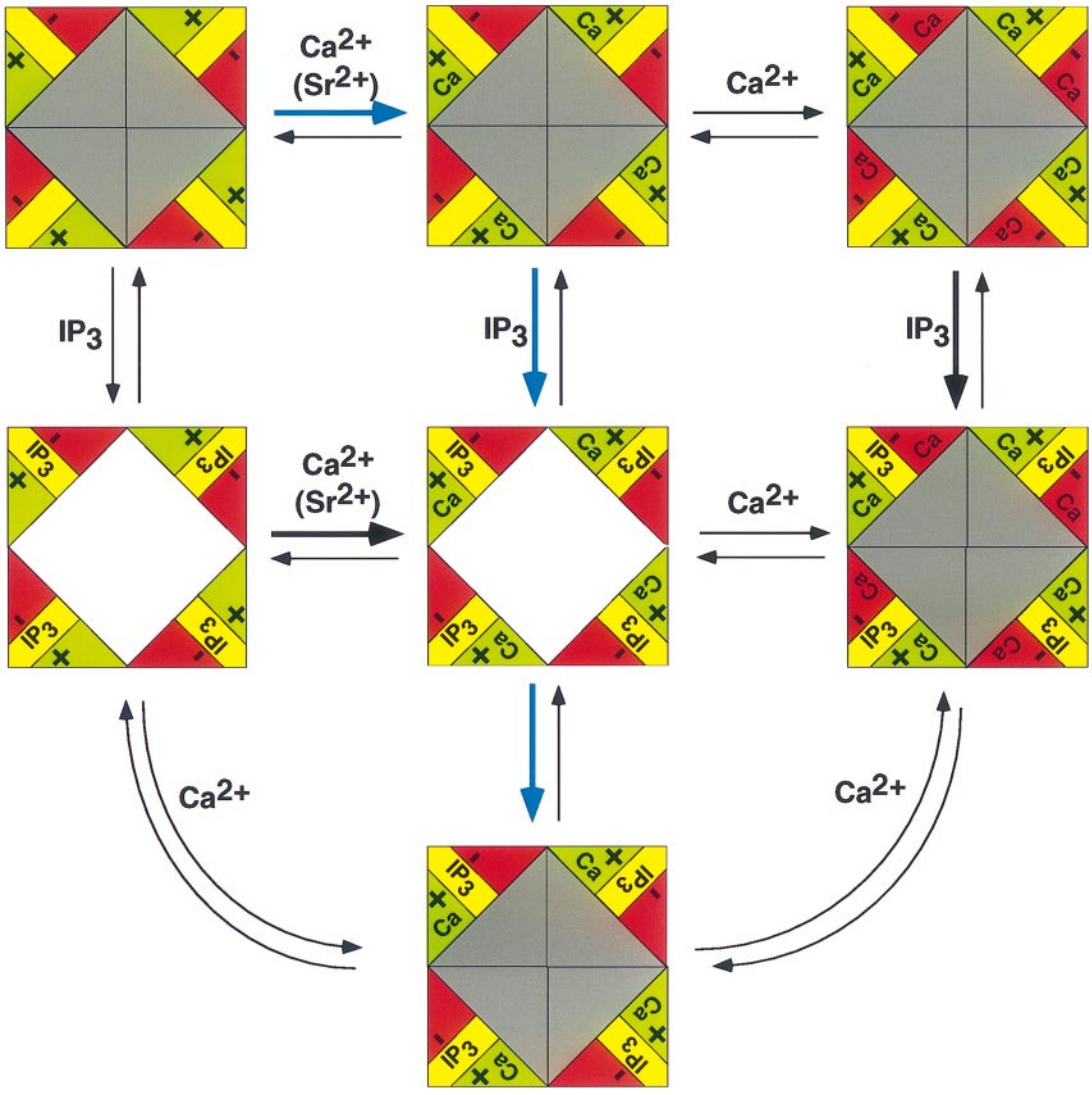


**Fig. 9.** Scheme showing coupled $Ca^{2+}$-dependent activation and inactivation of the $IP_3R$. Each subunit of the tetrameric $IP_3R$ is depicted with an $IP_3$-binding site (yellow), a site for stimulation by $Ca^{2+}$ (green) that increases $IP_3$ affinity and an inhibitory $Ca^{2+}$ site (red) that inactivates the channel independently of $IP_3$. The channel pore is shown in gray for closed and inactivated conformations, and as a clear white diamond where channel opening can occur. The scheme is arranged in three columns, the $Ca^{2+}$-unbound state at low $[Ca^{2+}]_c$ (left), the $IP_3$-sensitized state induced by submicromolar $[Ca^{2+}]_c$ levels (middle) and the inactivated state elicited by higher $[Ca^{2+}]_c$ (right). The predominant pathway of coupled $IP_3R$ activation and inactivation proposed here for the generation of a $[Ca^{2+}]_c$ spike is shown by the blue arrows.

ation of the ryanodine receptor by depolarization in skeletal muscle has also been reported (Pizarro *et al.*, 1996), suggesting that this may be a common property of intracellular $Ca^{2+}$ release channels. This process is ideally suited to generate a stable transient increment of $Ca^{2+}$ release during each $[Ca^{2+}]_c$ spike. In the final phase of the $[Ca^{2+}]_c$ oscillation cycle, the intrinsic inactivation, perhaps in combination with direct feedback inhibition by $[Ca^{2+}]_c$, allows a return to basal $[Ca^{2+}]_c$ through the action of $Ca^{2+}$ pumps. Recovery of the $IP_3R$ from $IP_3$-dependent inactivation can occur either by dissociation of $Ca^{2+}$ from the stimulatory site or by removal of $IP_3$ (Hajnóczky and Thomas, 1994) but, since $Ca^{2+}$ regulates $IP_3$ affinity, both $Ca^{2+}$ and $IP_3$ are expected to dissociate from the $IP_3R$ during the recovery phase. Although $IP_3R$ inactivation reverses more slowly than the direct inhibitory effect of $Ca^{2+}$ (Finch *et al.*, 1991; Ilyin and Parker, 1994; but cf. Oancea and Meyer, 1996), it is not slow enough to account for the long interspike periods. Therefore, other factors may be involved in resetting the system prior to the next $[Ca^{2+}]_c$ spike or, alternatively, the primary determinant of oscillation frequency may be the time required to generate a sufficient $Ca^{2+}$ trigger signal to initiate the next $Ca^{2+}$ release spike. Overall, the coupled feedback regulation of the $IP_3R$ by $Ca^{2+}$ and $IP_3$ is likely to play a key role in ensuring that the amplitude and duration of each $[Ca^{2+}]_c$ spike is constant over a range of $IP_3$ and agonist doses, to yield an essentially pure frequency-modulated $[Ca^{2+}]_c$ signal.

## Materials and methods

### *Imaging measurements in intact and permeabilized hepatocytes*

Hepatocytes were isolated from the livers of Sprague–Dawley rats by collagenase perfusion and maintained in primary culture for 3–24 h in Williams E medium, as described previously (Rooney *et al.*, 1989; Hajnóczky *et al.*, 1993), except that dexamethasone was omitted.

For measurements of $[Ca^{2+}]$, $[Sr^{2+}]$ and $[Ba^{2+}]$ in intact hepatocytes,

the cells were loaded with 5 μM fura2/AM for 15 min in the presence of 100 μM sulfinpyrazone or were microinjected with fura2 free acid as described previously (Rooney *et al.*, 1989; Lin *et al.*, 1994). Measurements of $Mn^{2+}$ quench of compartmentalized fura2 utilized cells loaded with 5 μM fura2/AM for 45–60 min (Renard-Rooney *et al.*, 1993; Hajnóczky *et al.*, 1994). Fura2 and other $Ca^{2+}$ indicators were loaded into intact hepatocytes incubated at 37°C in extracellular medium (ECM) composed of 121 mM NaCl, 5 mM $NaHCO_3$, 10 mM Na-HEPES, 4.7 mM KCl, 1.2 mM $KH_2PO_4$, 1.2 mM $MgSO_4$, 2 mM $CaCl_2$, 10 mM glucose and 2% bovine serum albumin (BSA), pH 7.4. Intact cell experiments were carried out in the same buffer with BSA reduced to 0.25%, and $CaCl_2$ was omitted for measurements of $Mn^{2+}$ quench and intracellular $[Sr^{2+}]$ and $[Ba^{2+}]$. The free $[Ca^{2+}]$ of this $Ca^{2+}$-free ECM was 400 nM measured using fura2 free acid (1.5 μM).

Measurements of $[Ca^{2+}]_{ER}$ in permeabilized hepatocytes were carried out by first loading the intact cells for 60–120 min with 6 μM furaptra/AM or 6 μM fura2FF/AM. These $Ca^{2+}$ indicators have $K_d$ values of 53 μM for furaptra (Hofer and Machen, 1994) and 35 μM for fura2FF (A.Minta, TEFLABS), making them suitable for measuring changes in $[Ca^{2+}]_{ER}$. Dye-loaded hepatocytes were washed with $Ca^{2+}$-free buffer and permeabilized by incubation for 6 min with 15 μg/ml digitonin in intracellular medium (ICM) composed of 120 mM KCl, 10 mM NaCl, 1 mM $KH_2PO_4$, 20 mM Tris-HEPES at pH 7.2 with 2 mM MgATP and 1 μg/ml each of antipain, leupeptin and pepstatin. In order to decrease $[Ca^{2+}]_o$, the ICM was passed through a Chelex column prior to addition of MgATP and protease inhibitors. Medium free $[Ca^{2+}]$ was <100 nM after Chelex treatment and did not exceed 300–400 nM after addition of ATP and protease inhibitors. Direct measurement of $[Ca^{2+}]_o$ using 250 nM fura2 in the imaging chamber in the presence of permeabilized hepatocytes yielded a free $[Ca^{2+}]$ of ~400 nM. In some experiments 2 μM CPT-cAMP was added to facilitate $IP_3R$ activation and $Ca^{2+}$ re-uptake (Hajnóczky *et al.*, 1993), since this appeared to increase the percentage of responsive cells, but all findings were reproduced in the absence of this agent. After permeabilization, the cells were washed into fresh buffer without digitonin. There was no detectable metabolism of $IP_3$ in the permeabilized cell preparation.

Individual cells were examined by digital imaging fluorescence microscopy at 35°C (Rooney *et al.*, 1989, 1990; Renard-Rooney *et al.*, 1993; Hajnóczky *et al.*, 1993, 1995). $[Ca^{2+}]_c$ in intact cells was calculated from the fluorescence ratio derived from image pairs obtained using 340 and 380 nm excitation. $Mn^{2+}$ quench of compartmentalized fura2 fluorescence was measured using the $Ca^{2+}$-insensitive excitation wavelength of 360 nm (Glennon *et al.*, 1992; Hajnóczky *et al.*, 1993, 1994). Calibration of fura2FF signals in permeabilized hepatocytes gave values of ~500 μM for $[Ca^{2+}]_{ER}$ after completion of ATP-dependent $Ca^{2+}$ uptake. Experiments were carried out with at least three different cell preparations, and 30–50 cells were monitored in each experiment. Submaximal $IP_3$ evoked $[Ca^{2+}]_{ER}$ oscillations in 50–60% of cells and stepwise $Mn^{2+}$ quench of compartmentalized fura2 in 25–30% of cells. Traces represent single cell responses unless indicated otherwise.

#### *Fluorometric measurements of ion fluxes in suspensions of permeabilized hepatocytes*

Suspensions of fura2-loaded hepatocytes were permeabilized with 25 μg/ml digitonin in the presence of 2 μM thapsigargin and 1 μM ruthenium red for 10 min at 37°C in a fluorometer cuvette (Deltascan, PTI), as described previously (Hajnóczky *et al.*, 1993, 1994; Renard-Rooney *et al.*, 1993; Hajnóczky and Thomas, 1994). For experiments where $[Ca^{2+}]_o$ was varied, EGTA (5–23 μM) and $CaCl_2$ (8 μM) were included during the pre-incubation. Actual $[Ca^{2+}]_o$ values were measured with the small amount of fura2 (~0.2 μM final) released from the cells. $MnCl_2$ (usually 60 μM) was added together with EGTA to give a constant level of $Ca^{2+}$ and $Mn^{2+}$ during the $Mn^{2+}$ uptake phase for all $[Ca^{2+}]_o$ pre-incubation conditions. The quench of luminal fura2 by $Mn^{2+}$ was monitored with 360 nm excitation. Dual wavelength excitation (340/380 nm) of compartmentalized fura2 fluorescence was used to monitor the entry of $Sr^{2+}$ and $Ba^{2+}$ into the stores, whereas single wavelength excitation at the appropriate isofluorescence wavelengths (365 nm for $Sr^{2+}$ and 370 nm for $Ba^{2+}$) was used to monitor $Mn^{2+}$ quench in the presence of these divalent cations. Although it might be expected that $Sr^{2+}$ or $Ba^{2+}$ in the stores would interfere with the $Mn^{2+}$ quenching of fura2, this effect was found to be negligible both by calculation of the expected binding of $Mn^{2+}$ in the presence and absence of these ions, and by direct measurements with fura2 *in vitro*. For example, addition of 0.8 μM $MnCl_2$ to fura2 (nominally 1.5 μM) quenched the fluorescence by 31.1 and 29.3% in the presence and absence of 60 μM $SrCl_2$, respectively. It should also be noted that the basal leak of $Sr^{2+}$ and $Ba^{2+}$ into the stores was sufficient to approach equilibration during the 90 s pre-incubation period, even in the absence of $IP_3$ (see Figure 7).

#### *[$^3$H]$IP_3$ binding measurements*

Hepatocytes were permeabilized at 2 mg of protein/ml in ICM. All studies with $Sr^{2+}$ and $Ba^{2+}$ and the $Ca^{2+}$ dependence of $IP_3$ binding were carried out in the presence of 40 μM EGTA and at 22°C. Incubations with [$^3$H]$IP_3$ (1.4 nM for 90 s) were carried out with $[Ca^{2+}]_o$ values set by addition of $CaCl_2$ (0–45 μM) or in the presence of 160 μM $Sr^{2+}$ or $Ba^{2+}$. The bound and free fractions were separated by filtration (GF/B filters, transit time 2–3 s). Non-specific binding determined in the presence of 10 μM unlabeled $IP_3$ was <5% of total binding. Specific binding was normalized to maximum binding attained in the presence of $Ca^{2+}$ (14.8 ± 1.5 fmol/mg cell protein). The time course of increased $IP_3$ binding induced by $Sr^{2+}$ was measured after 4 min pre-incubation with 50 nM [$^3$H]$IP_3$.

## Acknowledgements

This work was supported by grants DK38422 and DK51526 from the NIH. G.H. is a recipient of a Burroughs Wellcome Fund Career Award in the Biomedical Sciences.

## References

Berridge,M.J. (1990) Calcium oscillations. *J. Biol. Chem.*, **265**, 9583–9586.

Berridge,M.J. (1993) Inositol trisphosphate and calcium signalling. *Nature*, **361**, 315–325.

Berridge,M.J., Cobbold,P.H. and Cuthbertson,K.S. (1988) Spatial and temporal aspects of cell signalling. *Philos. Trans. R. Soc. Lond. B, Biol. Sci.*, **320**, 325–343.

Bezprozvanny,I., Watras,J. and Ehrlich,B.E. (1991) Bell-shaped calcium-response curves of Ins(1,4,5)$P_3$ and calcium-gated channels from endoplasmic reticulum of cerebellum. *Nature*, **351**, 751–754.

Chatton,J.-Y., Liu,H. and Stucki,J.W. (1995) Simultaneous measurements of $Ca^{2+}$ in the intracellular stores and the cytosol of hepatocytes during hormone-induced $Ca^{2+}$ oscillations. *FEBS Lett.*, **368**, 165–168.

Clapham,D.E. (1995) Calcium signaling. *Cell*, **80**, 259–268.

Cobbold,P.H., Sanchez-Bueno,A. and Dixon,C.J. (1991) The hepatocyte calcium oscillator. *Cell Calcium*, **12**, 87–95.

Combettes,L., Cheek,T.R. and Taylor,C.W. (1996) Regulation of inositol trisphosphate receptors by luminal $Ca^{2+}$ contributes to quantal $Ca^{2+}$ mobilization. *EMBO J.*, **15**, 2086–2093.

DeLisle,S. and Welsh,M.J. (1992) Inositol trisphosphate is required for the propagation of calcium waves in *Xenopus* oocytes. *J. Biol. Chem.*, **267**, 7963–7965.

Finch,E.A., Turner,T.J. and Goldin,S.M. (1991) Calcium as a coagonist of inositol 1,4,5-trisphosphate-induced calcium release. *Science*, **252**, 443–446.

Ghosh,T.K., Eis,P.S., Mullaney,J.M., Ebert,C.L. and Gill,D.L. (1988) Competitive, reversible, and potent antagonism of inositol 1,4,5-trisphosphate-activated calcium release by heparin. *J. Biol. Chem.*, **263**, 11075–11079.

Glennon,C.M., Bird,G.St.J., Kwan,C.Y. and Putney,J.W.,Jr (1992) Actions of vasopressin and the Ca($^{2+}$)-ATPase inhibitor, thapsigargin, on $Ca^{2+}$ signaling in hepatocytes. *J. Biol. Chem.*, **267**, 8230–8233.

Goldbeter,A., Dupont,G. and Berridge,M.J. (1990) Minimal model for signal-induced $Ca^{2+}$ oscillations and for their frequency encoding through protein phosphorylation. *Proc. Natl Acad. Sci. USA*, **87**, 1461–1465.

Hajnóczky,G. and Thomas,A.P. (1994) The inositol trisphosphate calcium channel is inactivated by inositol trisphosphate. *Nature*, **370**, 474–477.

Hajnóczky,G., Gao,E., Nomura,T., Hoek,J.B. and Thomas,A.P. (1993) Multiple mechanisms by which protein kinase A potentiates inositol 1,4,5-trisphosphate-induced $Ca^{2+}$ mobilization in permeabilized hepatocytes. *Biochem. J.*, **293**, 413–422.

Hajnóczky,G., Lin,C. and Thomas,A.P. (1994) Luminal communication between intracellular $Ca^{2+}$ stores modulated by GTP and the cytoskeleton. *J. Biol. Chem.*, **269**, 10280–10287.

Hajnóczky,G., Robb-Gaspers,L.D., Seitz,M.B. and Thomas,A.P. (1995) Decoding of cytosolic calcium oscillations in the mitochondria. *Cell*, **82**, 415–424.

Harootunian,A.L., Kao,J.P.Y., Paranjape,S. and Tsien,R.Y. (1991) Generation of calcium oscillations in fibroblasts by positive feedback between calcium and $IP_3$. *Science*, **251**, 75–78.

Hofer,A.M. and Machen,T.E. (1993) Technique for *in situ* measurement of calcium in intracellular inositol 1,4,5-trisphosphate-sensitive stores using the fluorescent indicator mag-fura-2. *Proc. Natl Acad. Sci. USA*, **90**, 2598–2602

Hofer,A.M. and Machen,T.E. (1994) Direct measurement of free Ca in organelles of gastric epithelial cells. *Am. J. Physiol.*, **267**, G442–G451.

Iino,M. (1990) Biphasic $Ca^{2+}$ dependence of inositol 1,4,5-trisphosphate-induced Ca release in smooth muscle cells of the guinea pig taenia caeci. *J. Gen. Physiol.*, **95**, 1103–1122

Ilyin,V. and Parker,I. (1994) Role of cytosolic $Ca^{2+}$ in inhibition of $InsP_3$-evoked $Ca^{2+}$ release in *Xenopus* oocytes. *J. Physiol.*, **477**, 503–509.

Kasai,H., Li,Y.X. and Miyashita,Y. (1993) Subcellular distribution of $Ca^{2+}$ release channels underlying $Ca^{2+}$ waves and oscillations in exocrine pancreas. *Cell*, **74**, 669–677.

Lechleiter,J.D. and Clapham,D.E. (1992) Molecular mechanisms of intracellular calcium excitability in *X.laevis* oocytes. *Cell*, **69**, 283–294.

Lin,C., Hajnóczky,G. and Thomas,A.P. (1994) Propagation of cytosolic calcium waves into the nuclei of hepatocytes. *Cell Calcium*, **16**, 247–258.

Marshall,I.C.B. and Taylor,C.W. (1993) Biphasic effect of cytosolic $Ca^{2+}$ on Ins(1,4,5)$P_3$-stimulated $Ca^{2+}$ mobilization in hepatocytes. *J. Biol. Chem.*, **268**, 13214–13220.

Marshall,I.C.B. and Taylor,C.W. (1994) Two calcium-binding sites mediate the interconversion of liver inositol 1,4,5-trisphosphate receptors between three conformational states. *Biochem. J.*, **301**, 591–598.

Meyer,T. and Stryer,L. (1991) Calcium spiking. *Annu. Rev. Biophys. Biophys. Chem.*, **20**, 153–174.

Meyer,T., Wensel,T. and Stryer,L. (1990) Kinetics of calcium channel opening by inositol 1,4,5-trisphosphate. *Biochemistry*, **29**, 32–37.

Missiaen,L., Taylor,C.W. and Berridge,M.J. (1991) Spontaneous calcium release from inositol trisphosphate-sensitive calcium stores. *Nature*, **352**, 241–244.

Missiaen,L., DeSmedt,H., Droogmans,G. and Casteel,R. (1992) $Ca^{2+}$ release induced by inositol 1,4,5-trisphosphate is a steady-state phenomenon controlled by luminal $Ca^{2+}$ in permeabilized cells. *Nature*, **357**, 599–602.

Montero,M., Brini,M., Marsault,R., Alvarez,J., Sitia,R., Pozzan,T. and Rizzuto,R. (1995) Monitoring dynamic changes in free $Ca^{2+}$ concentration in the endoplasmic reticulum of intact cells. *EMBO J.*, **14**, 5467–5475.

Morgan,A.J. and Jacob,R. (1996) $Ca^{2+}$ influx does more than provide releasable $Ca^{2+}$ to maintain repetitive spiking in human umbilical vein endothelial cells. *Biochem. J.*, **320**, 505–517.

Nunn,D.L. and Taylor,C.W. (1992) Luminal $Ca^{2+}$ increases the sensitivity of $Ca^{2+}$ stores to inositol 1,4,5-trisphosphate. *Mol. Pharmacol.*, **41**, 115–119.

Oancea,E. and Meyer,T. (1996) Reversible desensitization of inositol trisphosphate-induced calcium release provides a mechanism for repetitive calcium spikes. *J. Biol. Chem.*, **271**, 17253–17260.

Parker,I. and Ivorra,I. (1990) Inhibition by $Ca^{2+}$ of inositol trisphosphate-mediated $Ca^{2+}$ liberation: a possible mechanism for oscillatory release of $Ca^{2+}$. *Proc. Natl Acad. Sci. USA*, **87**, 260–264.

Petersen,O.H. and Wakui,M. (1990) Oscillating intracellular $Ca^{2+}$ signals evoked by activation of receptors linked to inositol lipid hydrolysis: mechanism of generation. *J. Membr. Biol.*, **118**, 93–105.

Pietri,F., Hilly,M. and Mauger,J.P. (1990) Calcium mediates the interconversion between two states of the liver inositol 1,4,5-trisphosphate receptor. *J. Biol. Chem.*, **265**, 17478–17485.

Pizarro,G., Shirokova,N., Tsugorka,A., Blatter,L.A. and Rios,E. (1996) Quantal release of calcium in skeletal muscle. *Biophys. J.*, **70**, A234.

Renard-Rooney,D.C., Hajnóczky,G., Seitz,M.B., Schneider,T.G. and Thomas,A.P. (1993) Imaging of inositol 1,4,5-trisphosphate-induced $Ca^{2+}$ fluxes in single permeabilized hepatocytes: demonstration of both quantal and nonquantal patterns of $Ca^{2+}$ release. *J. Biol. Chem.*, **268**, 23601–23610.

Robb-Gaspers,L.D. and Thomas,A.P. (1995) Coordination of $Ca^{2+}$ signaling by intercellular propagation of $Ca^{2+}$ waves in the intact liver. *J. Biol. Chem.*, **270**, 8102–8107.

Rooney,T.A., Sass,E.J. and Thomas,A.P. (1989) Characterization of cytosolic calcium oscillations induced by phenylephrine and vasopressin in single fura-2-loaded hepatocytes. *J. Biol. Chem.*, **264**, 17131–17141.

Rooney,T.A., Sass,E.J. and Thomas,A.P. (1990) Agonist-induced cytosolic calcium oscillations originate from a specific locus in single hepatocytes. *J. Biol. Chem.*, **265**, 10792–10796.

Rouxel,F.P., Hilly,M. and Mauger,J.P. (1992) Characterization of a rapidly dissociating inositol 1,4,5-trisphosphate-binding site in liver membranes. *J. Biol. Chem.*, **267**, 20017–20023.

Sanderson,M.J., Charles,A.C., Boitano,S. and Dirksen,E.R. (1994) Mechanisms and function of intercellular calcium signaling. *Mol. Cell. Endocrinol.*, **98**, 173–187.

Stauffer,P.L., Zhao,H., Luby-Phelps,K., Moss,R.L., Star,R.A. and Muallem,S. (1993) Gap junction communication modulates $[Ca^{2+}]_i$ oscillations and enzyme secretion in pancreatic acini. *J. Biol. Chem.*, **268**, 19769–19775.

Striggow,F. and Ehrlich,B.E. (1996) The inositol 1,4,5-trisphosphate receptor of cerebellum—$Mn^{2+}$ permeability and regulation by cytosolic $Mn^{2+}$. *J. Gen. Physiol.*, **108**, 115–124.

Tanimura,A. and Turner,J.R. (1996a) Calcium release in HSY cells conforms to a steady-state mechanism involving regulation of the inositol 1,4,5-trisphosphate receptor $Ca^{2+}$ channel by luminal $[Ca^{2+}]$. *J. Cell Biol.*, **132**, 607–616.

Tanimura,A. and Turner,R.J. (1996b) Inositol 1,4,5-trisphosphate-dependent oscillations of luminal $[Ca^{2+}]$ in permeabilized HSY cells. *J. Biol. Chem.*, **271**, 30904–30908

Thomas,A.P., Alexander,J. and Williamson,J.R. (1984) Relationship between inositol polyphosphate production and the increase of cytosolic free $Ca^{2+}$ induced by vasopressin in isolated hepatocytes. *J. Biol. Chem.*, **259**, 5574–5584.

Thomas,A.P., Bird,G.St.J., Hajnóczky,G., Robb-Gaspers,L.D. and Putney,J.W.,Jr (1996) Spatial and temporal aspects of cellular calcium signalling. *FASEB J.*, **10**, 1505–1517.

Thorn,P., Lawrie,A.M., Smith,P.M., Gallacher,D.V. and Petersen,O.H. (1993) Local and global cytosolic $Ca^{2+}$ oscillations in exocrine cells evoked by agonists and inositol trisphosphate. *Cell*, **74**, 661–668.

Toescu,E.C. (1995) Temporal and spatial heterogeneities of $Ca^{2+}$ signaling: mechanisms and physiological roles. *Am. J. Physiol.*, **269**, G173–G185.

Tse,A., Tse,F.W., Almers,W. and Hille,B. (1993) Rhythmic exocytosis stimulated by GnRH-induced calcium oscillations in rat gonadotropes. *Science*, **260**, 82–84.

Tse,F.W., Tse,A. and Hille,B. (1994) Cyclic $Ca^{2+}$ changes in intracellular stores of gonadotropes during gonadotropin-releasing hormone-stimulated $Ca^{2+}$ oscillations. *Proc. Natl Acad. Sci. USA*, **91**, 9750–9754.

Wakui,M., Potter,B.V.L. and Petersen,O.H. (1989) Pulsatile intracellular calcium release does not depend on fluctuations in inositol trisphosphate concentration. *Nature*, **339**, 317–320.

Woods,N.M., Cuthbertson,K.S. and Cobbold,P.H. (1986) Repetitive transient rises in cytoplasmic free calcium in hormone-stimulated hepatocytes. *Nature*, **319**, 600–602.

*Received on January 8, 1997; revised on March 6, 1997*